

Cite this: *Chem. Commun.*, 2014, 50, 7477

 Received 17th February 2014,  
 Accepted 27th May 2014

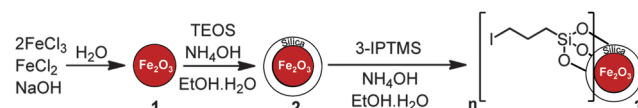
DOI: 10.1039/c4cc01250j

[www.rsc.org/chemcomm](http://www.rsc.org/chemcomm)

**Neocuproine has been covalently bound to silica-coated magnetite ( $\gamma$ -Fe<sub>2</sub>O<sub>3</sub>) magnetic nanoparticles (MNPs) by a phenyl ether linkage. The resulting MNPs are able to remove Cu(II) from 12 ppm aqueous solution with an extraction efficiency of up to 99% at pH 2.**

Magnetic nanoparticles (MNPs) combine high surface area with ease of separation<sup>1</sup> and the use of iron oxide particles has opened fascinating separation applications.<sup>2–7</sup> However, iron oxide based MNPs in combination with complexing agents cannot be used in acidic media, which would dissolve the particles.<sup>8</sup> A way to solve this problem is to use silica to provide a chemically unreactive surface whilst not affecting the core.<sup>8</sup> Furthermore, the free Si-OH surface groups can allow effective covalent binding of organic functional groups onto the surface of the SiO<sub>2</sub>-coated MNPs. Commonly, surface modification with alkoxy silanes of the general formula X-(CH<sub>2</sub>)<sub>n</sub>-Si(OR)<sub>3</sub>, is used where X represents the head-group functionality, (CH<sub>2</sub>)<sub>n</sub> that acts as a flexible spacer, and Si(OR)<sub>3</sub> the anchor group that can attach to the free Si-OH groups on the surface of the MNPs.<sup>9,10</sup> The present work combines the stability of SiO<sub>2</sub>-coated MNPs and the complexing power of neocuproine<sup>11</sup> in order to study the capabilities of such materials for the effective removal of Cu(II) from aqueous solutions at different pH.

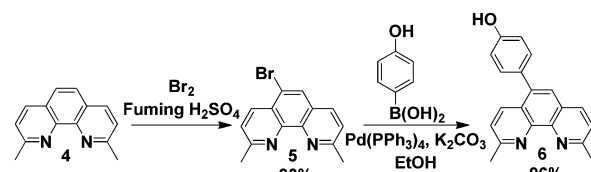
Iron oxide ( $\gamma$ -Fe<sub>2</sub>O<sub>3</sub>) MNPs were prepared by co-precipitation<sup>8,12–14</sup> from a 1:2 aqueous mixture of FeCl<sub>2</sub> and FeCl<sub>3</sub> with sodium hydroxide. The external silica layer was then coated onto the surface of the MNPs by a sol-gel method using tetraethyl orthosilicate (TEOS).<sup>8,12–14</sup> After this, the silica surface was further modified with 3-iodopropyltrimethoxysilane (3-IPTMS) (Scheme 1).



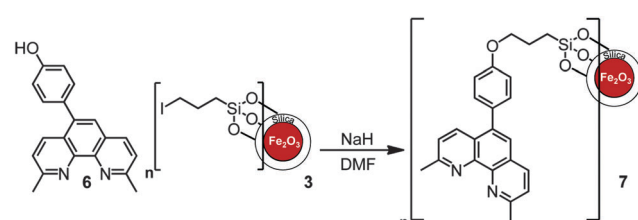
Scheme 1 Synthesis of iodoalkyl-functionalized SiO<sub>2</sub>-coated MNPs **3**.

In order to introduce functionality at the 5-position of neocuproine **4**, bromination<sup>15,16</sup> was carried out with bromine (0.6 equivalents) in the presence of fuming H<sub>2</sub>SO<sub>4</sub> (20% SO<sub>3</sub>). Replacement of the bromine with a 4-hydroxyphenol linking group was successfully achieved *via* Suzuki coupling<sup>17</sup> with 4-hydroxyphenylboronic acid (Scheme 2). This phenol functionalized ligand could then be immobilized onto the MNPs by nucleophilic substitution of the iodo-substituent (Scheme 3).

Each functionalization step of the MNPs was followed by infrared spectroscopy. Fig. 1 depicts the FT-IR spectra of uncoated ( $\gamma$ -Fe<sub>2</sub>O<sub>3</sub>) MNPs **1**, SiO<sub>2</sub>-coated MNPs **2** and iodoalkyl-functionalized SiO<sub>2</sub>-coated MNPs **3**. The  $\gamma$ -Fe<sub>2</sub>O<sub>3</sub> MNPs **1** cause



Scheme 2 Synthesis of 5-(4-hydroxyphenyl)-2,6-dimethyl-1,10-phenanthroline **6**.



Scheme 3 Immobilisation of neocuproine on MNPs.

<sup>a</sup> School of Chemistry, University of Reading, Whiteknights, Reading, Berkshire RG6 6AD, UK. E-mail: l.m.harwood@reading.ac.uk

<sup>b</sup> Environment Department, University of York, Heslington, York, YO10 5DD, UK

<sup>c</sup> Department of Geography and Environmental Science, University of Reading, Whiteknights, Reading, Berkshire RG6 6AD, UK

† Dedicated to Richard Taylor, a colleague and valued friend, to celebrate his 65th birthday.

‡ Electronic supplementary information (ESI) available: Experimental details and characterization of compounds. See DOI: 10.1039/c4cc01250j



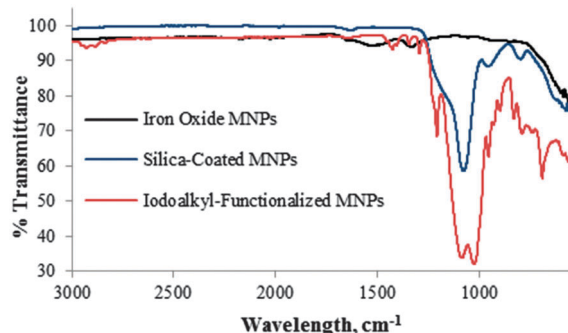


Fig. 1 FR-IR spectra of  $\text{Fe}_2\text{O}_3$  **1**,  $\text{SiO}_2$ -coated  $\text{Fe}_2\text{O}_3$  **2**, and iodoalkyl-functionalized  $\text{SiO}_2$ -coated MNPs **3**.

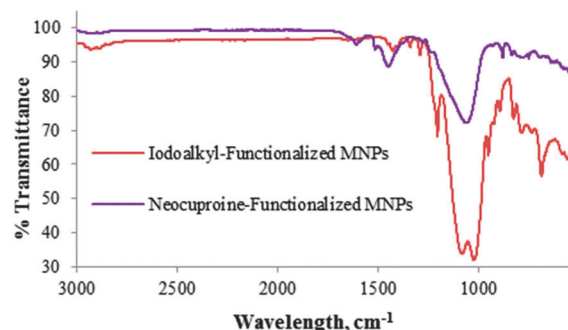


Fig. 2 FR-IR spectra of iodoalkyl-functionalized  $\text{SiO}_2$ -coated MNPs **3** and neocuproine-functionalized  $\text{SiO}_2$ -coated MNPs **7**.

two strong absorptions at 630 and 580  $\text{cm}^{-1}$ . The introduction of silica on the surface of the  $\gamma\text{-Fe}_2\text{O}_3$  MNPs **1** results in an additional absorption band at 1080  $\text{cm}^{-1}$  owing to Si–O stretching. After functionalization with 3-iodopropyltrimethoxysilane, bands at 2930  $\text{cm}^{-1}$  and 688  $\text{cm}^{-1}$  were observed, assigned to the C–H stretching and C–I stretching modes of iodoalkyl-functionalized  $\text{SiO}_2$ -coated MNPs **3**, respectively.

The FT-IR spectra shown in Fig. 2 demonstrate a clear distinction between iodoalkyl-functionalized  $\text{SiO}_2$ -coated MNPs **3** and neocuproine-functionalized  $\text{SiO}_2$ -coated MNPs **7**. Absence of the C–I stretching absorption at 688  $\text{cm}^{-1}$  and presence of bands at 1500–1600  $\text{cm}^{-1}$  owing to C=C aromatic vibrations are indicative of the covalent incorporation of neocuproine onto the MNPs.

The unfunctionalized  $\gamma\text{-Fe}_2\text{O}_3$  MNPs **1** were characterized by X-ray powder diffraction<sup>18</sup> and were found to consist of pure maghemite or  $\gamma\text{-Fe}_2\text{O}_3$ ,<sup>19</sup> whereas diffraction data of the composite nanoparticles after modification with silica did not show any well defined peaks (ESI‡), indicating that the silica coating is thick enough to interfere with the iron oxide diffraction, or the iron oxide is more amorphous than before (smaller particles, smaller diffracting domains or more disordered structure) allowing the silica pattern to dominate.

Representative TEM images of  $\gamma\text{-Fe}_2\text{O}_3$  MNPs **1**, iodoalkyl-functionalized  $\text{SiO}_2$ -coated MNPs **3** and neocuproine-functionalized  $\text{SiO}_2$ -coated MNPs **7**, shown in Fig. 3, were recorded on the particles dispersed in methanol and dried on a copper grid at room temperature.

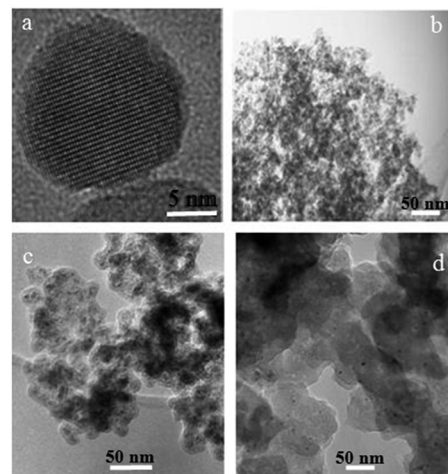


Fig. 3 TEM images of (a, b)  $\gamma\text{-Fe}_2\text{O}_3$  MNPs **1**, (c) iodoalkyl-functionalized  $\text{SiO}_2$ -coated MNPs **3** and (d) neocuproine functionalized MNPs **7**.

Fig. 3(a) shows the predominantly spherical morphology of the  $\gamma\text{-Fe}_2\text{O}_3$  MNPs **1** with an average diameter of *ca.* 15 nm. These tended to form aggregates as shown in Fig. 3(b). In the case of iodoalkyl-functionalized  $\text{SiO}_2$ -coated MNPs **3** [Fig. 3(c)], the diameter of the particles was found to be *ca.* 20–25 nm, while Fig. 3(d) reveals that neocuproine-functionalized  $\text{SiO}_2$ -coated MNPs **7** have diameter of *ca.* 50–55 nm.

To complement the TEM images that only provide information on the size of the MNP cores, DLS measurements (ESI‡) were also carried out. This indicated the  $\gamma\text{-Fe}_2\text{O}_3$  MNPs **1**, iodoalkyl-functionalized  $\text{SiO}_2$ -coated MNPs **3** and neocuproine-functionalized  $\text{SiO}_2$ -coated MNPs **7** to have narrow particle size distributions and average diameter values of 15, 48, and 72 nm, respectively. The values measured for the iodoalkyl-functionalized  $\text{SiO}_2$ -coated MNPs **3** and neocuproine-functionalized  $\text{SiO}_2$ -coated MNPs **7** are larger compared to the TEM images; this phenomenon has been observed previously.<sup>20,21</sup>

The organic content on the MNPs was investigated using thermal gravimetric analysis (TGA) under nitrogen. The weight loss for the  $\text{SiO}_2$ -coated MNPs **2** was about 2.5% over the temperature range from 60–200 °C, presumably due to the loss of residual water; whereas the TGA curve of iodoalkyl-functionalized  $\text{SiO}_2$ -coated MNPs **3** showed a sharp weight loss

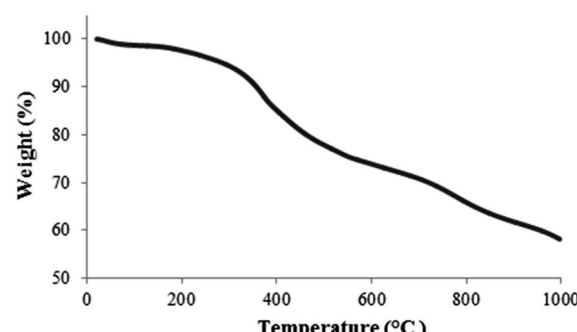


Fig. 4 TGA curve of MNPs **7**.



at 250–300 °C, proposed to correspond to the loss of iodoalkyl coating (ESI‡). The TGA curve (Fig. 4) of neocuproine-functionalized  $\text{SiO}_2$ -coated MNPs 7 shows three weight-loss steps. Below 200 °C, the weight loss is quite small, probably resulting from the removal of absorbed water. After that, there is a significant weight loss from 300–500 °C corresponding to the decomposition of the organic components. From this, it can be estimated that the amount of neocuproine bound onto the MNPs is about ~15% w/w (ESI‡). Further weight loss at 700–900 °C can be attributed to the formation of iron carbide.<sup>22,23</sup>

The extraction of Cu(II) from aqueous media was tested by weighing about 12 mg of functionalized MNPs 7 into plastic tubes containing 10 mL solutions of 12 ppm of Cu(II) at different pH. The mixtures were sonicated for 5 min and then shaken overnight. A neodymium permanent magnet was placed for 60 seconds beneath the tube to move the MNPs to the tube wall allowing the supernatant liquid to be decanted. After separation, the supernatant was subjected to quantitative elemental analysis by atomic absorption spectrometry.

Acidity of an aqueous solution is known to exert a profound influence on extraction efficiency of various ligands.<sup>5</sup> The effect of solution pH on Cu(II) extraction was investigated in the range pH 2–8. As shown in Fig. 5, close to 99% of Cu(II) was removed at pH 2 (initial concentration 12.33 ppm, final concentration 0.13 ppm); although the extraction efficiency decreased with increasing the pH. The lowest pH was then selected for kinetic studies where extraction was effectively complete after 5 min (ESI‡).

The percentage of Cu(II) extraction from a 12 ppm initial concentration with different amounts of neocuproine-functionalized MNPs 7 at pH 2 is presented in Fig. 6 and shows

**Table 1** Extraction of Cu(II) from aqueous solution at pH 2 by  $\text{SiO}_2$ -coated  $\text{Fe}_2\text{O}_3$  **2**, iodoalkyl-functionalized  $\text{SiO}_2$ -coated MNPs **3** and neocuproine functionalized MNPs **7**

Removal (%)	Iodoalkyl-functionalized $\text{SiO}_2$ -coated MNPs	Neocuproine functionalized MNPs
17	30	99

an almost linear correlation of Cu(II) extraction with the amount of MNPs 7 added.

To assess the chelating effect of the bound neocuproine in functionalized MNPs 7, the extraction efficiencies of  $\text{SiO}_2$ -coated  $\text{Fe}_2\text{O}_3$  MNPs **2** and iodoalkyl-functionalized  $\text{SiO}_2$ -coated MNPs **3** were also investigated at pH 2 and compared with the extraction efficiency of neocuproine functionalized MNPs **7** (Table 1).

The extraction efficiencies of  $\text{SiO}_2$ -coated  $\text{Fe}_2\text{O}_3$  MNPs **2** and iodoalkyl-functionalized  $\text{SiO}_2$ -coated MNPs **3** were found to be 17% and 30%, respectively; compared to the 99% extraction efficiency observed for neocuproine functionalized MNPs **7**. Thus, the majority of the extraction capacity of functionalized MNPs **7** is due to the bound neocuproine.

In summary, neocuproine functionalized MNPs **7** have been prepared and characterised. These MNPs have the advantages of high surface area and their ability to be separated from aqueous media magnetically. Their ability to extract Cu(II) from aqueous media has been investigated at varying pH, with the maximum extraction efficiency of Cu(II) by the MNPs being found to be 99% at pH 2. Extraction was complete within 5 min and about 12 mg of these MNPs were able to alter the concentration of Cu(II) in 10 mL of solution from 12.33 ppm to 0.13 ppm.

The authors acknowledge the EPSRC for financial support (A.A.). Use of the Chemical Analysis Facility (CAF) and Centre for Advanced Microscopy (CfAM) at the University of Reading is gratefully acknowledged. We also would like to thank Mr Michael Andrews, Dr Peter Harris and Miss Anne Dudley for their assistance with X-ray diffraction (XRD), Transmission Electron Microscopy (TEM) and Atomic Absorption (AA) measurements, respectively.

## Notes and references

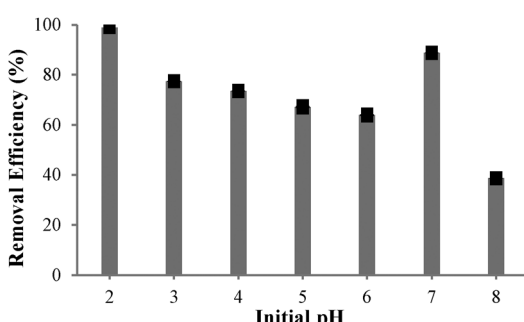


Fig. 5 Effect of initial pH on the extraction efficiency of Cu(II) by MNPs **7**.

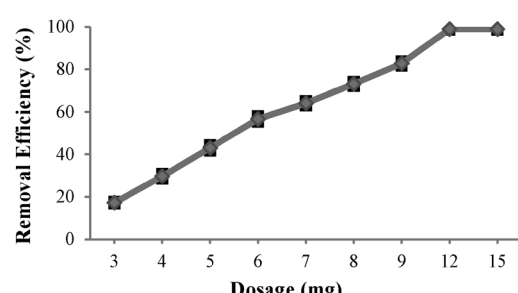


Fig. 6 Effect of MNPs **7** dosage on extraction of Cu(II).

- 1 A.-F. Ngomsik, A. Bee, D. Talbot and G. Cote, *Sep. Purif. Technol.*, 2012, **86**, 1–8.
- 2 Y. Sun, X. Ding, Z. Zheng, X. Cheng, X. Hu and Y. Peng, *Chem. Commun.*, 2006, 2765–2767.
- 3 F. M. Koehler, M. Rossier, M. Waelle, E. K. Athanassiou, L. K. Limbach, R. N. Grass, D. Gunther and W. J. Stark, *Chem. Commun.*, 2009, 4862–4864.
- 4 X. Liu, Q. Hu, Z. Fang, X. Zhang and B. Zhang, *Langmuir*, 2009, **25**, 3–8.
- 5 Y. Liu, M. Chen and H. Yongmei, *Chem. Eng. J.*, 2013, **218**, 46–54.
- 6 M. Kaur, A. Johnson, G. Tian, W. Jiang, L. Rao, A. Paszczynski and Y. Qiang, *Nano Energy*, 2013, **2**, 124–132.
- 7 M. H. Mashhadizadeh and Z. Karami, *J. Hazard. Mater.*, 2011, **190**, 1023–1029.
- 8 J. H. Jang and H. B. Lim, *Microchem. J.*, 2010, **94**, 148–158.
- 9 I. J. Bruce and T. Sen, *Langmuir*, 2005, **21**, 7029–7035.
- 10 M. Yamaura, R. L. Camilo, L. C. Sampaio, M. A. Macêdo, M. Nakamura and H. E. Toma, *J. Magn. Magn. Mater.*, 2004, **279**, 210–217.



11 P. Ashtari, K. Wang, X. Yang and S. J. Ahmadi, *Anal. Chim. Acta*, 2009, **646**, 123–127.

12 A. L. Morel, S. I. Nikitenko, K. Gionnet, A. Wattiaux, J. Lai-Kee-Him, C. Labrugere, B. Chevalier, G. Deleris, C. Petibois, A. Brisson and M. Simonoff, *ACS Nano*, 2008, **2**, 847–856.

13 M. Nazrul Islam, L. Van Phong, J.-R. Jeong and C. Kim, *Thin Solid Films*, 2011, **519**, 8277–8279.

14 F. W. Zhang, Z. Z. Zhu, Z. P. Dong, Z. K. Cui, H. B. Wang, W. Q. Hu, P. Zhao, P. Wang, S. Y. Wei, R. Li and J. T. Ma, *Microchem. J.*, 2011, **98**, 328–333.

15 J. Mlochowski, *Roczn. Chem.*, 1974, **48**, 2145–2155.

16 A. Afsar, D. M. Laventine, L. M. Harwood, M. J. Hudson and A. Geist, *Chem. Commun.*, 2013, **49**, 8534–8536.

17 J. P. W. Eggert, U. Luning and C. Nather, *Eur. J. Org. Chem.*, 2005, 1107–1112.

18 A. Afsar, D. M. Laventine, L. M. Harwood, M. J. Hudson and A. Geist, *Heterocycles*, 2014, **88**, 613–620.

19 T. Hyeon, S. S. Lee, J. Park, Y. Chung and H. B. Na, *J. Am. Chem. Soc.*, 2001, **123**, 12798–12801.

20 L. Sun, C. Huang, T. Gong and S. Zhou, *Mater. Sci. Eng., C*, 2010, **30**, 583–589.

21 J. Lim, S. Yeap, H. Che and S. Low, *Nanoscale Res. Lett.*, 2013, **8**, 381.

22 R. Snovski, J. Grinblat, M.-T. Sougrati, J.-C. Jumas and S. Margel, *J. Magn. Magn. Mater.*, 2014, **349**, 35–44.

23 M. Sharma, S. Mantri and D. Bahadur, *J. Magn. Magn. Mater.*, 2012, **324**, 3975–3980.

